Journal of Alloys and Compounds 508 (2010) 400–405

Contents lists available at ScienceDirect

Journal of Alloys and Compounds

journal homepage: www.elsevier.com/locate/jallcom

# Sonochemical synthesis and characterization of magnetic separable $Fe_3O_4$/Ag composites and its catalytic properties

Xueping Zhang[a], Wanquan Jiang[a,*], Xinglong Gong[b,*], Zhong Zhang[c]

[a] Department of Chemistry, University of Science and Technology of China (USTC), Hefei 230026, PR China
[b] CAS Key Laboratory of Mechanical Behavior and Design of Materials, Department of Modern Mechanics, USTC, Hefei 230027, PR China
[c] National Center for Nanoscience and Technology, Beijing 100080, PR China

ARTICLE INFO

*Article history:*
Received 27 May 2010
Received in revised form 9 August 2010
Accepted 15 August 2010
Available online 26 August 2010

*Keywords:*
Sonochemical
$Fe_3O_4$/Ag composites
Recyclable catalysts
RhB

ABSTRACT

A $Fe_3O_4$/Ag composite, with high efficiency in the degradation of rhodamine B was synthesized through a simple sonochemical method. These composites were obtained from sonication of $Ag(NH_3)_2^+$ and (3-aminopropyl)triethoxysilane (APTES)-coated $Fe_3O_4$ nanoparticles solution at room temperature in ambient air for 1 h. A formation mechanism was proposed and discussed. This sonochemical method is attractive since it eliminated the use of any reductants, which is necessary to transform the $Ag^+$ to the $Ag^0$. In comparison to high temperature or high pressure experimental processes, this method is mild, inexpensive, green and efficient. The M–H hysteresis loop of these $Fe_3O_4$/Ag composite microspheres indicates that the composite spheres exhibit superparamagnetic characteristics at room temperature. Furthermore, these composites can be recycled six times by magnetic separation without major loss of activity. Thus, these $Fe_3O_4$/Ag composites can be served as effective and convenient recyclable catalysts for practical application.

Crown Copyright © 2010 Published by Elsevier B.V. All rights reserved.

## 1. Introduction

Nanosized noble metal particles have attracted much attention due to unique optical, magnetic and electric properties from their bulk counterpart. In recent years, lots of works have focused on the application of these noble metal nanoparticles and were widely demonstrated in the literature [1–7]. For example, Zhao et al. prepared PS/Ag microspheres for microwave absorbing and 70% of the incident wave was absorbed by this nanoscale silver microwave absorbing coating [5]. Rather et al. reported that Ag/CNTs composites showed enhanced hydrogen storage capacity [6]. Gutes et al. opened up opportunities for the quantitative and in-field chemical trace analysis using silver nanodesert rose substrates [7]. It has been extensively demonstrated that nanosized metal particles have high catalytic activities for degradation of toluene, NO reduction, CO oxidation for their very large surface-to-volume ratio [8–10]. However, metal-nanoparticle catalysts would encounter an obstacle when applied in practice, that is, the difficulties in separating the products and residual catalysts with traditional methods such as centrifugation or filtration [11]. Therefore, the immobilization of metal nanocatalysts has attracted a lot of attention. Among various support materials, magnetic-nanoparticle supports are of particular interest because they permit the catalysts to be recovered efficiently by applying an external magnetic field.

Up to now, many methods have been established for synthesis of metal nanoparticles, including vapor deposition [12], chemical reactions [13], electroless plating [14]. However, more work is still needed to simplify the synthesis method. As a competitive alternative, the sonochemical method has been widely used to fabricate nanoparticles with unusual or improved properties. The physiochemical effects of ultrasound arise from acoustic cavitation, that is, the formation, growth and implosive collapse of bubbles in liquid. The implosive collapse of bubbles in liquid can accelerate many chemical reactions. Hence it offers a very attractive method for synthesis and application of various nanocomposites [15–20]. For example, Dang et al. synthesized magnetite nanoparticles with improved magnetic properties by sonochemistry [15]. Salavati-Niasari et al. reported a sonochemistry method to synthesize $Dy_2(CO_3)_3{\cdot}xH_2O$ nanoparticles which brought forward a broad idea to synthesize other rare-earth compounds with various morphologies and novel properties [16].Wang et al. synthesized $MnO_2$/MWNTs by sonochemistry and applied in hydrazine detection [17]. However, to date, no work has been reported on the synthesis of $Fe_3O_4$/Ag magnetic composites via an in situ sonochemistry method.

In this work, a simple, facile and speedy sonochemical method was developed to synthesize $Fe_3O_4$/Ag composites by three step reactions. First, $Fe_3O_4$ nanoparticles were prepared by conventional co-precipitation method. Second, the as-prepared $Fe_3O_4$

* Corresponding authors. Tel.: +86 551 3607605; fax: +86 551 3600419.
*E-mail addresses:* jiangwq@ustc.edu.cn (W. Jiang), gongxl@ustc.edu.cn (X. Gong).

0925-8388/$ – see front matter. Crown Copyright © 2010 Published by Elsevier B.V. All rights reserved.
doi:10.1016/j.jallcom.2010.08.070

nanoparticles were functionalized with functional amine group by APTES [(3-aminopropyl) triethoxysilane]. Third, $Ag^+$ was reduced to $Ag^0$ by sonication without using any reductant. The catalytic activity of the as-prepared composites for RhB degradation was also investigated. The $Fe_3O_4$/Ag composites was characterized using X-ray diffraction (XRD), transmission electron microscopy (TEM) with energy dispersive spectroscopy (EDS), X-ray photoelectron spectra (XPS), UV/vis absorption spectrum (UV–vis), and vibrating sample magnetometer (VSM).

## 2. Experimental section

### 2.1. Reagents and instruments

Ferric chloride hexahydrate ($FeCl_3 \cdot 6H_2O$, AR), Ferrous chloride tetrahydrate ($FeCl_2 \cdot 4H_2O$, AR), sodium borohydride ($NaBH_4$), Sodium hydroxide (NaOH), hydrochloric acid (HCl), rhodamine B (RhB, AR) from Sinopharm Chemical Reagent Co., Ltd (China). (3-aminopropyl) triethoxysilane (APTES) was purchased from Sigma (USA). Silver nitrate ($AgNO_3$), ammonium hydroxide ($NH_3 \cdot H_2O$, 25%–28%) from Lingfeng Chemical Reagent Co., Ltd of Shanghai (China). All reagents were used as received without further purification.

X-ray powder diffraction (XRD) patterns of the products were obtained with a Japan Rigaku DMax-γA rotation anode X-ray diffractometer equipped with graphite monochromatized Cu $K_\alpha$ radiation ($\lambda = 0.154178$ nm). Transmission electron microscopy (TEM) photographs were taken on a Hitachi Model H-800 TEM at an accelerating voltage of 200 kV. The high-resolution transmission electron microscopy (HR-TEM) images were taken on a JEOL-2010 TEM. X-ray photoelectron spectra (XPS) were measured on an ESCA Laboratory MKII instrument with Mg $K_\alpha$ radiation as the exciting source. The UV/vis spectra were registered by a UV-365 spectrophotometer.

### 2.2. Preparation of $Fe_3O_4$/Ag nanoparticles

The $Fe_3O_4$ nanoparticles were prepared through the conventional chemical co-precipitation of Fe(II) and Fe(III) chlorides ($Fe^{II}/Fe^{III}$ ratio = 0.5) with 1.5 M NaOH reported previously [21]. The black precipitate was magnetically separated and washed several times with water and ethanol. Finally, $Fe_3O_4$ microspheres were dispersed in ethanol to form 5 g/l solution.

For the modification of $Fe_3O_4$ nanoparticles with APTES, 25 ml of the above solution was diluted to 150 ml with absolute ethanol and 1 ml of $H_2O$ and sonicated for 30 min. After that, 0.4 ml of APTES was added with rapid stirring, and then the reaction solution was stirred at room temperature for 7 h. After being separated by a magnet, the resulting composites were washed several times with water and ethanol, and then dried under vacuum at 50 °C.

0.05 g of $Fe_3O_4$/APTES composite microspheres were dispersed in 100 ml of 2.9 mM $Ag(NH_3)_2^+$ solution and the solution was stirred for 30 min to ensure the adsorption of $Ag(NH_3)_2^+$ by the $Fe_3O_4$/APTES composite microspheres. Then, the reaction mixture was irradiated with a high-intensity ultrasonic probe (from Xinzhi Co., China, JY92–2D, with a 6 mm diameter titanium horn of 20 kHz working in a pulsed mode with a duty cycle of 7 s) at room temperature in ambient air for 1 h. After irradiation, the temperature of the reaction solution was about 60 °C. The resulting dark materials were separated by a magnet. The precipitated products were washed several times with water and ethanol and finally dried under vacuum at 50 °C.

### 2.3. The catalytic properties of the obtained $Fe_3O_4$/Ag composites

A given amount of $Fe_3O_4$/Ag composite microspheres were well dispersed in an aqueous solution containing RhB, and the volume of the mixture was adjusted to 30 ml with distilled water. Then, 10 ml of $NaBH_4$ solution was rapidly injected under stirring. The color of the reaction mixture gradually vanished, indicating the degradation of the dye solution. Changes in the concentration of RhB were monitored by measuring the variations in main absorbance peak (at 553 nm) in UV–vis spectra.

The recyclable efficiency of the catalysts was examined by repeating the same experiment. 0.01 g of $Fe_3O_4$/Ag composites were used to catalyze RhB ($[RhB] = 2 \times 10^{-5}$ mol/l, $[NaBH_4] = 1 \times 10^{-2}$ mol/l). After each cycle of degradation experiment was completed, the catalysts were separated by an external magnetic field, then followed by another "repeat". The recyclable catalytic efficiency was determined by measuring the absorption peak of RhB at the end of the catalytic reaction.

## 3. Results and discussion

### 3.1. The characterization of $Fe_3O_4$/Ag composites

Fig. 1 shows the typical TEM images of the as-prepared $Fe_3O_4$ nanoparticles, which clearly indicates that most of the particles are quasi-square and with an average diameter of 10 nm. After the sonication-assistant process, $Fe_3O_4$/Ag composites were obtained. Fig. 2 shows the TEM and HR-TEM images of $Fe_3O_4$/Ag composites. As observed from Fig. 2a, $Fe_3O_4$ nanocrystal and Ag nanocrystal in the composites cannot be distinguished. HR-TEM was used to further investigate the structure information of $Fe_3O_4$/Ag composites (Fig. 2b), which revealed that this sample was highly crystallized, as evidenced by the well-defined lattice fringes. The fringes of $d = 0.23$ nm match the (1 1 1) plane of Ag nanocrytsal, while the fringes of $d = 0.29$ nm match the (2 2 0) plane of $Fe_3O_4$ nanocrytsal, respectively. The HR-TEM results confirmed that $Fe_3O_4$ and Ag coexisted in the hybrid composite. Furthermore, an interconnected nanoparticular morphology was observed in Fig. 2b, which indicated a $Fe_3O_4$/Ag nanocrystal heterojunction was formed in the composite.

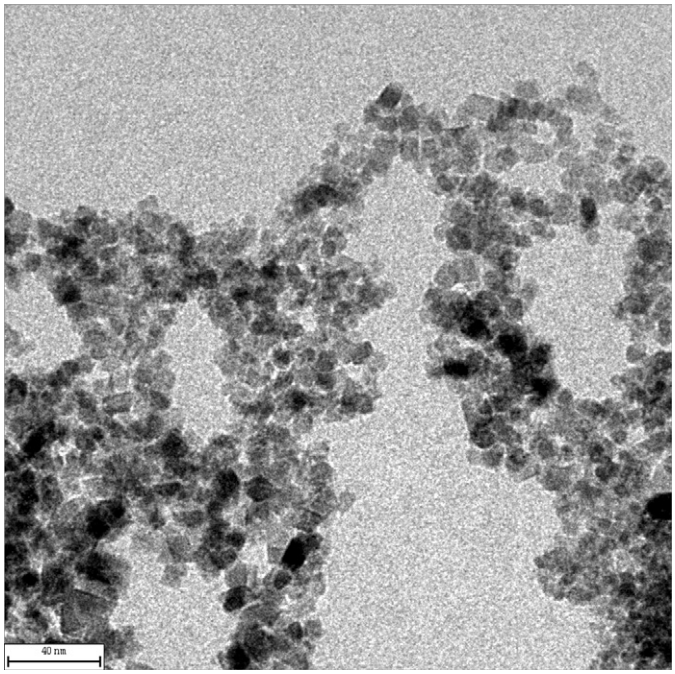


**Fig. 1.** TEM images of $Fe_3O_4$ nanoparticles.

To confirm the composition of the composites, EDS spectrum in situ composition analysis were collected and the result is shown in Fig. 3. EDS result indicated the presence of silver, iron, and silicon in the composites. The peaks of silver, iron, and silicon come from the Ag coating, $Fe_3O_4$ magnetic core, and the Si–O group of the APTES, which indicate that the iron oxide nanoparticles have been coated by Ag nanoparticles. However, in comparison to the peaks of Fe element, signal of Ag element was a little weaker. According to the above analysis, it could be concluded Ag/$Fe_3O_4$ hybrid nanocomposites have been successfully synthesized using such a sonochemistry method.

XPS analysis was conducted to further elucidate the surface composition of these particles, and the representative results are shown in Fig. 4. For $Fe_3O_4$, the main peaks are C1 s, Fe2p, and O1 s centered at 285 eV, 710.96 eV, 530.16 eV. In the spectrum of $Fe_3O_4$/APTES, new peaks appear at 101.65 eV and 399.71 eV, assigned to Si and N element on the surface of $Fe_3O_4$, which come from the Si–O and $-NH_2$ groups in APTES. Fig. 4c shows the XPS survey spectra of $Fe_3O_4$/Ag composites. The composites exhibit a new $Ag^0$ 3d peak (379.2 eV) which is very distinct from that of the $Fe_3O_4$ spheres and $Fe_3O_4$/APTES composites. This signal, which is not observed in the other two spectra, is in response to the Ag content in the composites. After the deposition of silver, the signal of Fe2p decreased from (18.24% atom) to (13.17% atom). However,

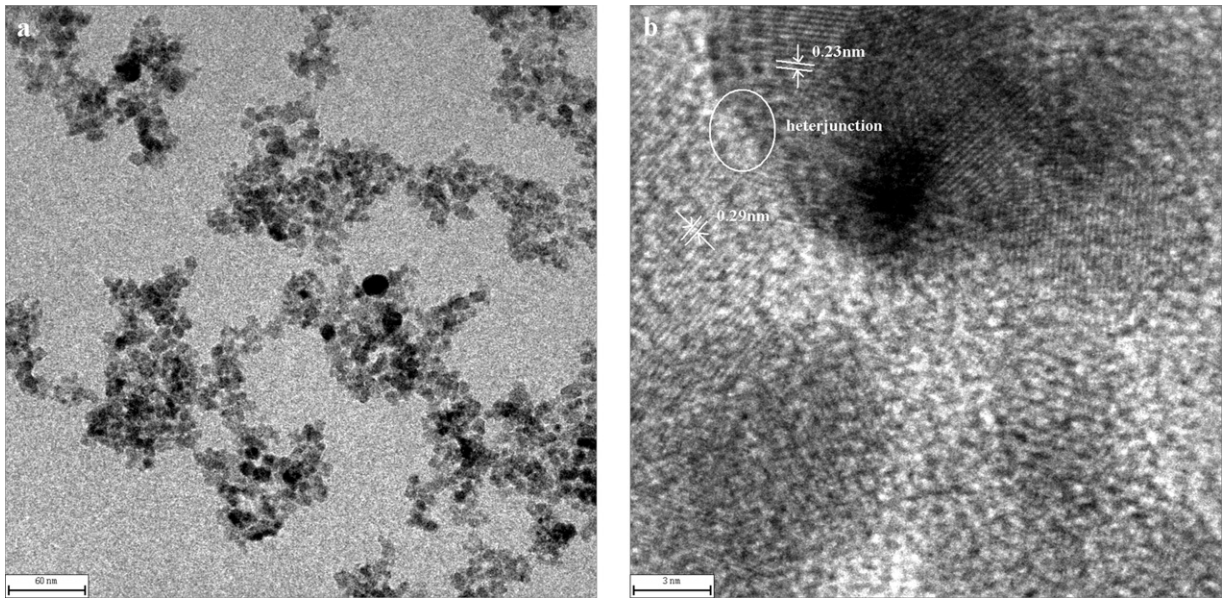


**Fig. 2.** (a) TEM images of $Fe_3O_4$/Ag composites. (b) HR-TEM images of $Fe_3O_4$/Ag composites.

there is still considerable residual signal of Fe2p in the spectrum of $Fe_3O_4$/Ag composites. These results suggested that $Fe_3O_4$ and Ag were present mainly as separated phases in $Fe_3O_4$/Ag composites, respectively.

In order to study the stability of the as-prepared composite catalysts, the samples of $Fe_3O_4$/Ag before and after catalytic reaction were subjected to XRD. As shown in Fig. 5, all of the diffraction peaks match well with Ag (JCPDS No. 03-0921) crystal and $Fe_3O_4$ crystal (JCPDS No. 75-0033). It can be seen that peaks of both Ag and $Fe_3O_4$ become a little weaker in Fig. 5b compared with Fig. 5a, which indicates that a small portion of crystal has been lost during the process of catalytic reaction. That is why in the recyclable experiments, the catalytic activity of composite catalysts decreased more or less during the degradation reaction. Processed water was also conducted ICP-AES analysis after catalysis reaction. As a result, it was found that about 0.033 μg/ml Ag was in the processed water, which meant Ag was stable enough to stay attached to the $Fe_3O_4$/APTES. Therefore, it could be concluded that the catalyst is stable.

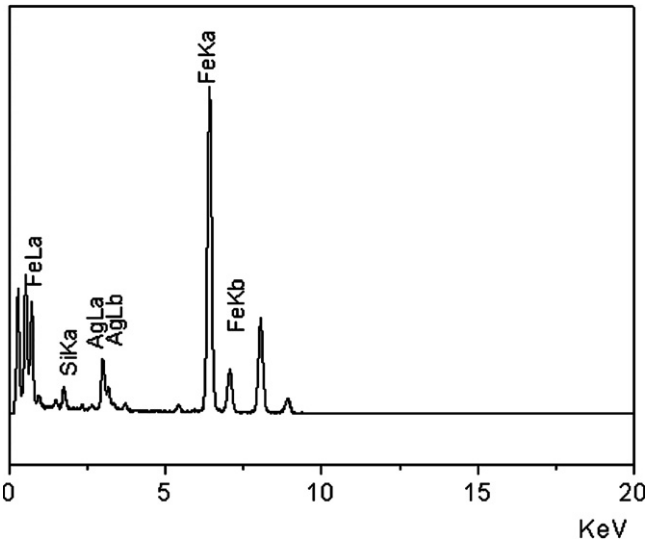


**Fig. 3.** EDS spectrum of $Fe_3O_4$/Ag composites.

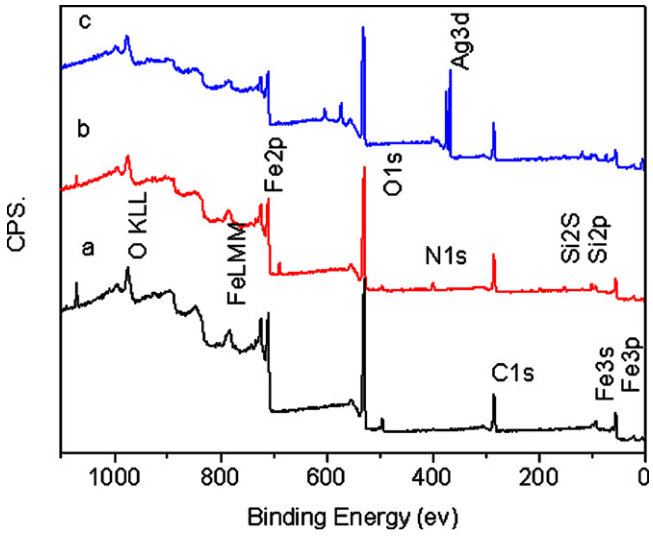


**Fig. 4.** XPS spectra of (a) $Fe_3O_4$ microspheres, (b) $Fe_3O_4$/APTES microspheres, and (c) $Fe_3O_4$/Ag composites microspheres.

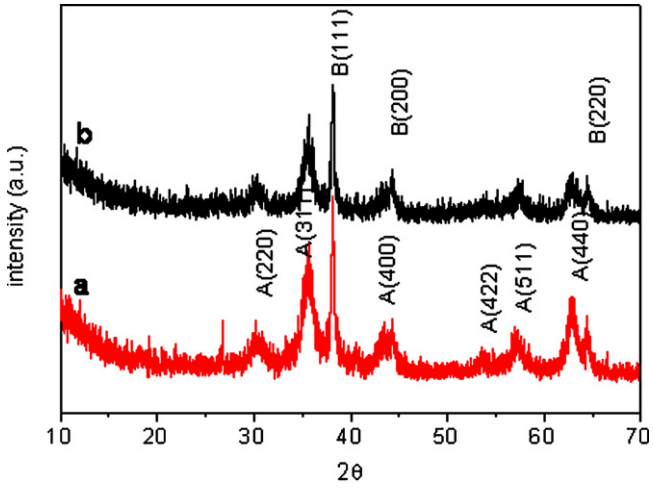


**Fig. 5.** X-ray diffraction patterns of $Fe_3O_4$/Ag before (a) and after (b) catalytic reaction.

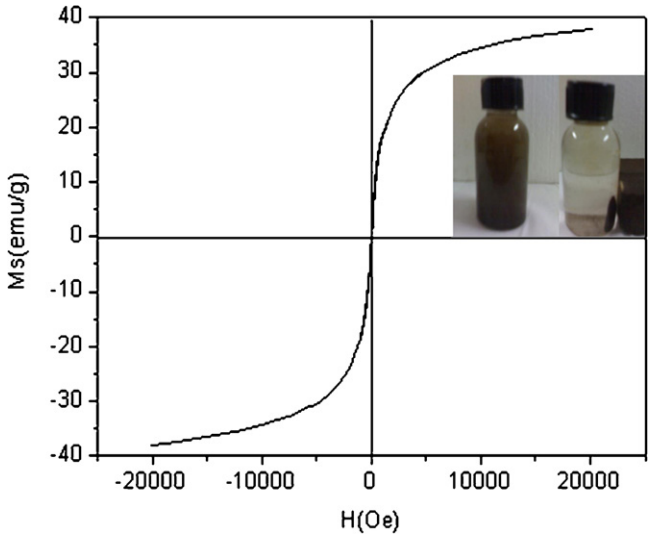


**Fig. 6.** M–H curve of $Fe_3O_4$/Ag composites at room temperature.

The M–H curve of the samples is shown in Fig. 6, in which the composites exhibit a superparamagnetic behavior without the observation of coercivity and remanence. With superparamagnetic property, the composite catalysts can be rapidly recovered by imparting an external magnetic field. The inset of Fig. 6 illuminated the effective model of catalysts separation and redispersion under an external magnetic field. Thus, the $Fe_3O_4$ nanoparticles are very appropriate as catalyst supports for separation and redispersion.

### 3.2. Proposed mechanism

For the synthesis of composite materials, $Fe_3O_4$ nanoparticles were functionalized with APTES. The previous work has demonstrated that the hydroxyl groups on the magnetite surface reacted with the ethoxy groups of the APTES molecules leading to the formation of Si–O bonds and leaving the terminal $-NH_2$ groups available for immobilization of silver [22]. The APTES-coated $Fe_3O_4$ nanoparticles show strong combination ability for silver metal ($Ag^+$ ions) by the long pair of terminal $-NH_2$ groups of organic entities. Thus Ag will attach on the surface of APTES-modified $Fe_3O_4$ nanoparticles by high-intensity ultrasound, which causing the reduction of $Ag^+$ reaction to be effected fast, accelerating the speed of silver depositing onto the APTES-coated $Fe_3O_4$ nanoparticle surface.

The chemical reaction ($Ag^+$ to $Ag^0$) can be driven by powerful ultrasound, which is strong enough to generate oxidation, reduction, dissolution, and decomposition [23–25]. Three different regions are formed in the aqueous sonochemical process: (i) the gas phase within the cavitation bubble, where elevated temperature (several thousand degrees) and high pressure (hundreds of atmosphere) are produced; (ii) the interfacial zone between the bubble and the bulk solution where the temperature is lower than that inside the bubble but still high enough for a sonochemical reaction; and (iii) the bulk solution at ambient temperature where reaction still takes place. In our case, of the aforementioned three regions, the interfacial zone was the preferred region where the reduction of $Ag(NH_3)_2{}^+$ occurred mainly because of the low vapor pressure of the reactants [26]. The likely reaction steps for the formation of Ag nanoparticles are as follows:

$$H_2O \xrightarrow{)))))} H^\bullet + OH^\bullet \quad (1)$$

$$2Ag(NH_3)_2{}^+ + H^\bullet \rightarrow 2Ag_{(S)} + (NH_4)^+ + NH_3 \quad (2)$$

As a result, Ag nanoparticles were immobilized on the surface of APTES-coated $Fe_3O_4$. Ag nanoparticles were obtained directly by sonication without any reductants, such as sodium borohydride and hexamethyle tetramine. There are two main advantages compared with the conventional methods to synthesize the similar structure [27–29]. One is the elimination of use of any reductant, and the other is the low temperature and short reaction time required in the sonochemical preparation. Therefore, this method has been proven to be simple, green, facile and inexpensive and can be used as an attractive alternative to prepare nanocomposites with tailored and unique properties.

### 3.3. The catalytic properties of as-prepared $Fe_3O_4$/Ag catalysts

Previous results demonstrated that Ag particles in nanoscale exhibited catalytic activity on a number of organic dyes, such as rhodamine B (RhB), methylene blue (MB) and eosin (EO) [30]. To evaluate the catalytic ability of $Fe_3O_4$/Ag composites, RhB dye solution was selected as the model. The choice of RhB is based on the following two factors. First, RhB, as a typical dye, represents a large class of environmental harmful compounds. Second, the RhB dye has different colors during the process of reduction period, so that the concentration of RhB can be examined by UV/vis absorption spectrum conveniently. Therefore, as a typical example of organic pollutants, investigation on the degradation of RhB has become very common with regard to the purification of dye effluents. The temporal UV/vis spectral change of RhB during catalytic reduction at the $Fe_3O_4$/Ag solution is shown in Fig. 7. As observed from Fig. 7, with the increase of the reaction time, the main absorbance of RhB gradually decreased, which indicated the reduction of RhB. As expected, the catalytic reduction of RhB proceeded successfully, and no deactivation or poisoning of the catalysts was observed. The blank experiment without $Fe_3O_4$/Ag composites have been carried out for reduction of the organic dye using the $NaBH_4$ solution. Experiment result showed that the degradation efficiency of RhB was just 7.6% after 60 min reduction (Table 1), indicating that the reduction of RhB by $NaHB_4$ did not occur to an appreciable extent in the absence of the Ag nanoparticles. This demonstrates that Ag nanoparticles play a key role in the catalytic reduction of RhB. According to earlier work [27], the catalysis process is through an electrochemical mechanism, where $Fe_3O_4$/Ag is intermediate between that of an oxidant and a reductant, and electron transfer occurs via the supported Ag nanoparticles. Dyes are electrophilic, while $BH_4{}^-$ ions are nucleophilic in nature with respect to silver nanoparicles. The catalytic reduction of RhB with various concentrations of catalysts is shown in Fig. 7. Evidently, with the increase of concentration of $Fe_3O_4$/Ag solution, the rate of the reduction of RhB increased, indicating that the reduction rate of RhB was significantly concentration-dependent. It is obviously observed that the degradation time of RhB for three different volumes of $Fe_3O_4$/Ag solution 1 ml, 1.4 ml, 2 ml are 25 min, 20 min and 12 min, respectively. Therefore, it is a feasible way to increase the mass of catalyst to improve the catalytic efficiency.

The magnetic properties of $Fe_3O_4$/Ag composite catalysts play an important role in efficient recovery and recycling of the catalysts. Due to the superparamagnetic property of the $Fe_3O_4$/Ag

**Table 1**
Degradation efficiency of RhB by $NaHB_4$ in the absence of $Fe_3O_4$/Ag.

| Degradation efficiency (%) | | | | | | |
|---|---|---|---|---|---|---|
| 0 | 10 | 20 | 30 | 40 | 50 | 60 (min) |
| 0 | 1.2 | 2.3 | 3.0 | 4.1 | 7.0 | 7.6 |

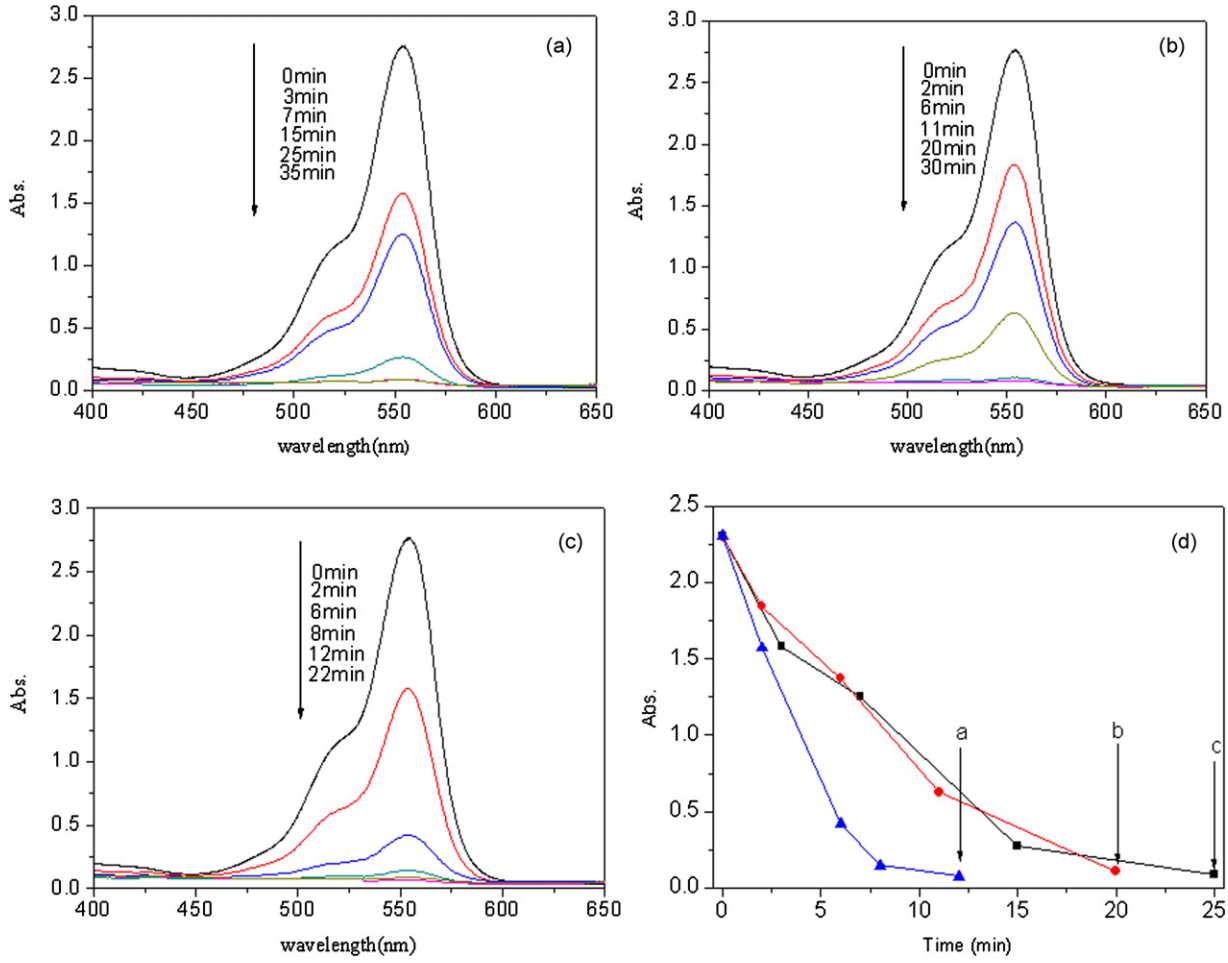


**Fig. 7.** UV–vis spectra of RhB during the degradation catalyzed by $Fe_3O_4$/Ag, [RhB] = $4 \times 10^{-5}$ mol/l. The arrows mark the increase of the reaction time. (a) 1 ml $Fe_3O_4$/Ag, (b) 1.4 ml $Fe_3O_4$/Ag, (c) 2 ml $Fe_3O_4$/Ag, (d) Curves of abs–time at different concentrations of catalyst (a: 1 ml; b: 1.4 ml; c: 2 ml $Fe_3O_4$/Ag solution).

nanoparticles, upon an external magnetic field, the magnetic composites were rapidly regathered and the rest of solution became clean within 1 min. As a practical recyclable catalysts, highly catalytic activity in each cycle of usage is necessary. The renewability of the catalysts was investigated. As indicated in Fig. 8, the catalytic activity of magnetic composites exhibited no significant decrease after six cycles of catalytic experiments. However, 85% of RhB is decomposed in the last cycle. In conclusion, the as-prepared composites have good catalytic ability in the degradation of RhB and this catalytic ability still maintain 87% even after being reused for 6 times. The decrease of catalytic activity after six cycles of usage may partly result from the incomplete separation of catalyst powders or the loss of catalysts during the degradation reaction. Thus, these magnetic catalysts can be used as ideal candidates in practical application.

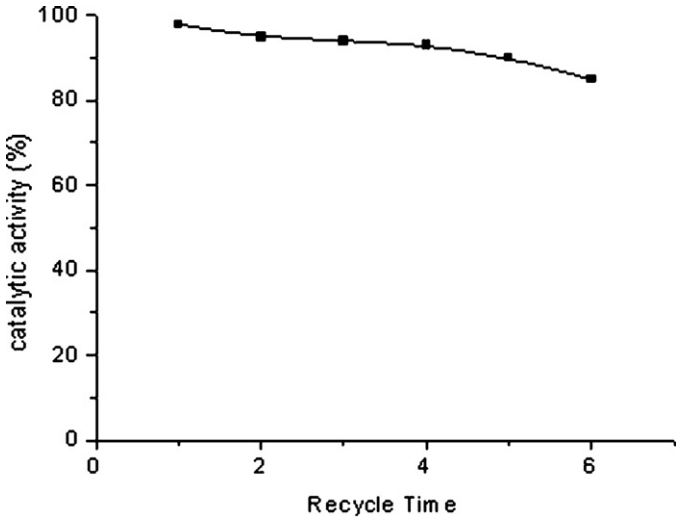


**Fig. 8.** Recycle experiments of the degradation reaction of RhB catalyzed by $Fe_3O_4$/Ag.

## 4. Conclusions

In summary, a simple sonochemical method for the synthesis of $Fe_3O_4$/Ag composites was reported. $Ag^+$ was reduced directly to $Ag^0$ by high-intensity ultrasound. This method is simple, facile, inexpensive and efficient compared with other routes to fabricate similar structure. The products display excellent magnetic properties at room temperature, and have good catalytic activity in the degradation of RhB. The renewable catalytic activity decreases slightly after each cycle of usage; however, 85% of RhB is decomposed in the last cycle, which means that the as-prepared composites can be used as convenient recyclable catalysts. Thus, this effective approach is expected to be used as attractive alternative to prepare other composites with tailored and unique properties.

## Acknowledgements

Financial support from National Basic Research Program of China (973 Program, Grant No. 2007CB936800) and SRFDP of China (Project No. 20093402110010) are gratefully acknowledged.

## References

[1] P. Sangpoura, O. Akhavana, A.Z. Moshfegha, J. Alloys Compd. 486 (2009) 22–28.
[2] J.G. Liu, X.Y. Li, X.Y. Zeng, J. Alloys Compd. 494 (2010) 84–87.
[3] H. Liu, B. Wang, E.S.P. Leong, P. Yang, Y. Zong, G.Y. Si, J.H. Teng, S.A. Maier, Nano 4 (2010) 3139–3146.
[4] K. Drozdowicz-Tomsia, F. Xie, E.M. Goldy, J. Phys. Chem. C 114 (2010) 1562–1569.
[5] W. Zhao, Q.Y. Zhang, H.P. Zhang, J.P. Zhang, J. Alloys Compd. 473 (2009) 206–211.
[6] S. Rathera, M. Naika, S.W. Hwanga, A.R. Kimb, K.S. Nahma, J. Alloys Compd. 475 (2009) L17–L21.
[7] A. Gutes, C. Carraro, R. Maboudia, Appl. Mater. Interfaces 1 (2009) 2551–2555.
[8] N. Li, F. Gaillard, Appl. Catal. B-Environ. 88 (2009) 152–159.
[9] P. Miquel, P. Granger, N. Jagtap, S. Umbarkarc, M. Dongare, C. Dujardin, J. Mol. Catal. A-Chem. (2010) 90–97.
[10] X. Bokhimi, R. Zanella, A. Morales, J. Phys. Chem. C 112 (2008) 12463–12467.
[11] M. Shokouhimehr, Y.Z. Piao, J. Kim, Y.J. Jang, T. Hyeon, Angew. Chem. Int. Ed. 46 (2007) 7039–7043.
[12] C.M. Ruan, G. Eres, W. Wang, Z.Y. Zhang, B.H. Gu, Langmuir 23 (2007) 5757–5760.
[13] M.W. Shao, L. Lu, H. Wang, S. Wang, M.L. Zhang, D.D. Ma, S.T. Lee, Chem. Commun. (2008) 2310–2312.
[14] Z.J. Wu, S.H. Ge, M.H. Zhang, W. Li, K.Y. Tao, J. Colloid Interface Sci. 330 (2009) 359–366.
[15] F. Dang, N.Y. Enomoto, J. Hojo, K.J. Enpuku, Ultrason. Sonochem. 16 (2009) 649–654.
[16] M. Salavati-Niasari, J. Javidi, F. Davar, A.A. Fazl, J. Alloys Compd. 503 (2010) 500–506.
[17] M.F. Wang, C. Wang, G.F. Wang, Electroanalysis 22 (2010) 1123–1129.
[18] W.Z. Lv, B. Liu, Q. Qiu, F. Wang, Z. Luo, P.X. Zhang, S.H. Wei, J. Alloys Compd. 479 (2009) 480–483.
[19] L.Q. Zhu, H. Zhang, W.P. Li, H.C. Liu, J. Alloys Compd. 471 (2009) 481–487.
[20] Q. Xiao, S.P. Huang, J. Zhang, C. Xiao, X.K. Tan, J. Alloys Compd. 459 (2008) L18–L22.
[21] Y.S. Kang, S. Risbud, J.F. Rabolt, P. Stroeve, Chem. Mater. 8 (1996) 2209–2211.
[22] Z.J. Jiang, C.Y. Liu, J. Phys. Chem. B 107 (2003) 12411–12415.
[23] J.Z. Sostaric, P. Mulvaney, F. Grieser, J. Chem. Soc. Faraday Trans. 91 (1995) 2843–2846.
[24] A.E. Alegria, Y. Lion, T. Kondo, P. Riesz, J. Phys. Chem. 93 (1989) 4908–4913.
[25] K.S. Suslick, M.M. Fang, T. Hyeon, J. Am. Chem. Soc. 118 (1996) 11960–11961.
[26] P. Jeevanandam, Y. Koltypin, Y. Mastai, A. Gedanken, J. Mater. Chem. 10 (2000) 2143–2146.
[27] Z.J. Jiang, C.Y. Liu, L.W. Sun, J. Phys. Chem. B 109 (2005) 1730–1735.
[28] A. Henglein, Chem. Mater. 10 (1998) 444–450.
[29] C.F. Jiang, M.W. Chen, S.H. Xuan, W.Q. Jiang, X.L. Gong, Z. Zhang, Can. J. Chem. 87 (2009) 502–506.
[30] N.R. Jana, T.K. Sau, T. Pal, J. Phys. Chem. B 103 (1999) 115–121.